Inorganica Chimica Acta 396 (2013) 49–59

Contents lists available at SciVerse ScienceDirect

Inorganica Chimica Acta

journal homepage: www.elsevier.com/locate/ica

Employment of pyridyl oximes and dioximes in zinc(II) chemistry: Synthesis, structural and spectroscopic characterization, and biological evaluation

Konstantis F. Konidaris [a], Maria Giouli [b], Catherine P. Raptopoulou [c], Vassilis Psycharis [c], Ioannis I. Verginadis [b], Anastasios Vasiliadis [d], Amalia S. Afendra [d], Spyridon Karkabounas [b,*], Evy Manessi-Zoupa [a,*], Theocharis C. Stamatatos [a,e,*]

[a] Department of Chemistry, University of Patras, 265 04 Patras, Greece
[b] Department of Physiology, Faculty of Medicine, University of Ioannina, 451 10 Ioannina, Greece
[c] Institute of Materials Science, NCSR "Demokritos", 153 10 Aghia Paraskevi Attikis, Greece
[d] Department of Biological Applications and Technologies, University of Ioannina, 451 10 Ioannina, Greece
[e] Department of Chemistry, Brock University, St. Catharines, Ontario, Canada L2S 3A1

ARTICLE INFO

Article history:
Received 12 August 2012
Accepted 27 September 2012
Available online 11 October 2012

Keywords:
Mononuclear Zn(II) complexes
Pyridyl oximes and dioximes
Crystal structures
Physicochemical characterization
Cytotoxic activity
Apoptosis

ABSTRACT

The employment of pyridine-2-amidoxime (ampaoH), 2,6-diacetylpyridine dioxime ($dapdoH_2$) and pyridine-2,6-diamidoxime ($dampdoH_2$) in zinc(II) chemistry is reported. The syntheses, crystal structures, spectroscopic and physicochemical characterization, and biological evaluation are described of $[Zn(O_2CMe)_2(ampaoH)_2]$ (**1**), $[Zn(O_2CPh)_2(ampaoH)_2]$ (**2**), $[Zn(dapdoH_2)_2](NO_3)_2$ (**3**) and $[Zn(dampdoH_2)_2](NO_3)_2$ (**4**). The reactions between $Zn(NO_3)_2{\cdot}4H_2O$ and two equivalents of either $dapdoH_2$ or $dampdoH_2$ in MeOH led to the mononuclear, cationic complexes **3** or **4**, respectively. The Zn^{II} center in **3** and **4** is coordinated by two *N*,*N*′,*N*″-tridentate chelating (η^3) $dapdoH_2$ or $dampdoH_2$ ligands, and it thus possesses a distorted octahedral coordination geometry. Strong intermolecular hydrogen bonding interactions provide appreciable thermodynamic stability and interesting supramolecular chemistry for compounds **1**–**4**. The characterization of all four complexes with ^1H and ^{13}C NMR, and positive ion electrospray mass spectroscopies confirmed their integrity in DMSO solutions. The biological evaluation of complex **3** showed the highest cytotoxic activity against LMS and MCF-7 cells, among the other three complexes (**1**, **2** and **4**). Flow cytometry analysis revealed that all four complexes cause apoptosis to LMS cells, at a dose-dependent manner. The combined work demonstrates the ability of pyridyl monoxime and pyridyl dioxime chelates not only to lead to polynuclear 3d-metal complexes with impressive structural motifs and interesting magnetic and optical properties, but also to yield new, mononuclear transition metal complexes with biological implications.

1. Introduction

Pyridyl oximes with the general formula (py)C(R)NOH (R = various) constitute a very important class of compounds related to biological systems. The strong nucleophilicity of the oximate anion, $\geq C{=}NO^-$, is associated with many hydrolytic processes, such as the transfer or cleavage of an acyl, phosphoryl or a sulfuryl group, by attacking an electrophilic center [1]. Among these actions, the fact that a series of pyridyl oximes have the ability to reactivate the enzyme acetylcholinesterase (AChE), when it is fully inhibited by organophosphorus compounds (OPs), including pesticides and chemical warfare agents, is of particular pharmacological interest [2]. OPs exert their acute toxicity through entire inhibition of AChE by forming covalently attached phosphorus conjugates with the hydroxyl group of the catalytic serine residue [3]. The reactivator is able to cleave the covalent bond between the OP and AChE, restoring activity of the enzyme. This reactivation process consists of an attack of the nucleophilic oximate anion on the P–O bond [4]. The most effective oximes used for treatment of OPs poisoning are the monopyridinium oxime Pralidoxime (2-PAM) and bispyridinium mono- or bis-oximes (Obidoxime, HI-6, Trimedoxime, etc.) [4,5]. Furthermore, a broad spectrum of biological activity of derivatives of pyridyl oximes has been investigated, such as activity on cardiovascular system, sedative, antidepressant and antispasmodic activity, analgesic and anti-inflammatory activity, among others [6].

On the other hand, there is currently a renewed interest in the coordination chemistry of pyridyl oximes whose anions are versatile ligands for a variety of objectives, including bridging affinity

* Corresponding authors. Address: Department of Chemistry, Brock University, St. Catharines, Ontario, Canada L2S 3A1. Tel.: +1 905 688 5550 (Th.C. Stamatatos), +30 2610 997 147 (E. Manessi-Zoupa), +30 26510 07576 (S. Karkabounas).
E-mail addresses: skarkabu@cc.uoi.gr (S. Karkabounas), emane@upatras.gr (E. Manessi-Zoupa), tstamatatos@brocku.ca (T.C. Stamatatos).

0020-1693/$ - see front matter © 2012 Elsevier B.V. All rights reserved.
http://dx.doi.org/10.1016/j.ica.2012.09.039

and formation of polynuclear metal complexes (clusters), isolation of coordination polymers, mixed-metal chemistry and significant magnetic characteristics [7,8]. From the bioinorganic point of view, the complexation of a metal ion with a pyridyloximate ligand would help the nucleophilicity of the oximate anion by lowering the pK of the molecule in an extent near the physiological values. This situation has been the starting point for a number of researchers, to create functional models of hydrolytic metalloenzymes. The first report concerning the hydrolytic activity of a metal/pyridyloxime complex belongs to R. Breslow and D. Chipman, about 50 years ago [9], who have studied the formation and hydrolytic activity of the moiety $[Zn\{(2\text{-py})C(H)NO\}]^+$. This compound combines the actions of the metal ion for the substrate binding and the coordinated oxime as the nucleophile. The extension of this work, with the study of the catalytic activity of the conjugation of a metal ion/pyridyloxime/cyclodextrine, has led to the biomimetic chemistry term "artificial enzyme" [10]. In this context, Zn(II) complexes with pyridine-2-carbaldehyde oxime or methyl 2-pyridyl ketone oxime [11] and 3d-metal complexes of 2,6-diacetylpyridine dioxime [12] have been studied kinetically for ester hydrolysis.

It is furthermore known that metal complexes of biologically active compounds possess features of considerable pharmaceutical interest because of several factors. In fact, the field of medicinal inorganic chemistry emerged a long time ago [13], and it is based on certain principles such as: (a) complexation with a non-labile metal protects the drug against enzymatic degradations because of the inertness of certain metal–ligand linkages, (b) the metal complex can have better hydrophobicity/hydrophilicity properties than the free ligand and, through this, it can improve the transport processes in the tissues, (c) the metal complex can release the active drug(s) in a specific organ, and its activity can be reinforced by the combination of effects from the ligands and from the metal residue [14]. Worldwide research based on these principles is focused on the design of metal-based drugs [14,15].

Zinc is an essential trace metal for various biological processes, involving an interaction with nucleic acids, an integral component of more than 200 enzymes and the major regulatory ion in the metabolism of cells. Additionally, in brain, zinc also acts as neuromodulator [16]. Some Zn(II) compounds have shown potent cytotoxic activity against various cancer cell lines [17], significant antibacterial and antifungal activities [18], as well as antidiabetic activities [19]. Despite the essential biological role of the labile Zn^{II} ion and its natural use in the active site of many hydrolytic enzymes, the coordination chemistry of this metal ion with various pyridyl oximes is poorly explored. Some years ago, our group has started a program aiming at the systematic investigation of the Zn^{II}/pyridyloxime system by means of exploring the structural and chemical characteristics of the new complexes, the study of their physicochemical properties (i.e. luminescence) and the evaluation of their biological properties [20–22]. Given the broad biological activity of pyridyl oximes, we herein report the synthesis, structures, and physicochemical and cytotoxic activity of four new Zn(II) complexes bearing the pyridyloxime and pyridyl dioxime ligands (Fig. 1), pyridine-2-amidoxime (ampaoH), 2,6-diacetylpyridine dioxime ($dapdoH_2$) and pyridine-2,6-diamidoxime ($dampdoH_2$).

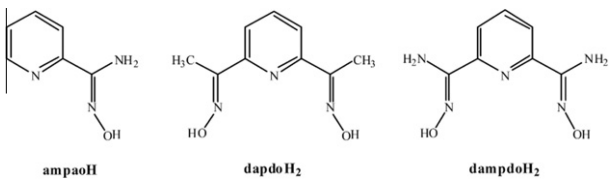

Fig. 1. General structural formula and abbreviations of the organic ligands discussed in the text.

2. Experimental

2.1. General and physical measurements

All manipulations were performed under aerobic conditions using materials (reagent grade) and solvents as received. The free ligands ampaoH, $dapdoH_2$ and $dampdoH_2$ were synthesized according to the literature methods [23–25]. The preparation of complexes $[Zn(O_2CMe)_2(ampaoH)_2]$ (**1**) and $[Zn(O_2CPh)_2(ampaoH)_2]$ (**2**) has been previously reported in detail by some of us [26].

Infrared (IR) spectra were recorded in the solid state (KBr pellets) on a Perkin-Elmer 16 PC FT spectrometer in the 4000–400 cm^{-1} range. Elemental analyses (C, H, and N) were performed by the in-house facilities of the University of Patras using an EA 1108 Carlo Erba analyser. The ^1H and ^{13}C NMR spectra of the structurally new complexes **3** and **4** in DMSO-d_6 were recorded with a Bruker Avance 400 MHz spectrometer; chemical shifts are reported relative to tetramethylsilane. Electrospray ionization (ESI) mass spectra were taken on a 7T-Fourier-transform ion cyclotron resonance (FT-ICR) mass spectrometer (APEX II, Bruker Daltonik) from solutions of complexes **1**–**4** prepared in DMSO.

2.2. Compound preparation

2.2.1. $[Zn(dapdoH_2)_2](NO_3)_2$ (**3**)

To a colorless solution of $Zn(NO_3)_2{\cdot}4H_2O$ (0.13 g, 0.50 mmol) in MeOH (10 mL) was slowly added a solution of $dapdoH_2$ (0.19 g, 1.00 mmol) in the same solvent (10 mL). The resulting colorless solution was kept under stirring at room temperature for about 20 min, filtered, and the filtrate was layered with Et_2O (40 mL). Slow mixing gave after 3 days well-formed, X-ray quality colorless prismatic crystals of **3**. The crystals were collected by filtration, washed with cold MeOH (2 × 3 mL) and Et_2O (2 × 5 mL), and dried in air. Typical yields were in the 80–85% range. *Anal.* Calc. for $C_{18}H_{22}ZnN_8O_{10}$: C, 37.6; H, 3.9; N, 19.5. Found: C, 37.8; H, 4.0; N, 19.3%. IR data (KBr pellet, cm^{-1}): ν = 3450mb, 3270sb, 3096m, 1634m, 1596s, 1570m, 1472s, 1384vs, 1316s, 1280s, 1202m, 1142m, 1046vs, 964m, 918 m, 810s, 740m, 696s, 668m, 520 m. ^1H NMR (400 MHz, DMSO-d_6): δ 12.55 (s, 2H, NO-H), 7.95 (d, J = 7.35, 2H, py-3(5)H), 8.12 (t, J = 7.30, 1H, py-4H), 2.43 (s, 6H, $-CH_3$). ^{13}C NMR (400 MHz, DMSO-d_6): δ 157.35 (–C=NOH), 155.85 (py-1(6)C), 136.15 (py-4C), 118.51 (py-3(5)C), 10.12 (-CH_3).

2.2.2. $[Zn(dampdoH_2)_2](NO_3)_2{\cdot}4H_2O$ (**4**$\cdot 4H_2O$)

To a colorless solution of $Zn(NO_3)_2{\cdot}4H_2O$ (0.13 g, 0.50 mmol) in MeOH (10 mL) was slowly added a solution of $dampdoH_2$ (0.20 g, 1.00 mmol) in the same solvent (10 mL). The resulting pale yellow solution was kept under stirring at room temperature for about 10 min, filtered, and the filtrate was layered with Et_2O (40 mL). Slow mixing gave after 5 days well-formed, X-ray quality colorless prismatic crystals of **4**$\cdot 4H_2O$. The crystals were collected by filtration, washed with cold MeOH (2 × 3 mL) and Et_2O (2 × 5 mL), and dried in air. Typical yields were in the 60–65% range. The air-dried solid was analyzed as solvent-free **4**. *Anal.* Calc. for $C_{14}H_{18}ZnN_{12}O_{10}$: C, 29.0; H, 3.1; N, 29.0. Found: C, 28.8; H, 3.0; N, 29.1%. IR data (KBr pellet, cm^{-1}): ν = 3442mb, 3342sb, 2920m, 2856m, 1660vs, 1604m, 1586m, 1492w, 1402m, 1384vs, 1328s, 1094m, 1032m, 1010m, 912w, 816m, 742m, 708m, 666m, 534m. ^1H NMR (400 MHz, DMSO-d_6): δ 12.58 (s, 2H, NO–H), 7.90 (d, J = 7.32, 2H, py-3(5)H), 8.10 (t, J = 7.28, 1H, py-4H), 5.45 (s, 4H, $-NH_2$), 2.35 (s, 6H, $-CH_3$). ^{13}C NMR (400 MHz, DMSO-d_6): δ 158.25

(–C=NOH), 156.25 (py-1(6)C), 137.42 (py-4C), 119.30 (py-3(5)C), 10.23 ($–CH_3$).

2.3. Single-crystal X-ray crystallography

The crystallographic data and structure refinement details for complexes **1** and **2** have been previously reported [26], whereas the corresponding data for the two structurally new compounds **3** and **4**·4H_2O are summarized in Table 1. A prismatic colorless crystal of **3** was mounted in a capillary, while a prismatic colorless crystal of **4**·4H_2O was mounted in air. Diffraction measurements for both complexes **3** and **4**·4H_2O were performed on a Rigaku R-AXIS SPIDER Image Plate diffractometer using graphite-monochromated Cu Kα radiation. Data collection (ω-scans) and processing (cell refinement, data reduction and empirical absorption correction) were performed using the CrystalClear program package [27a]. Both structures were solved by direct methods using SHELXS-97 [27b] and refined on F^2 by full-matrix least squares techniques with SHELXL-97 [27c]. The crystal of complex **3** is a pseudo merhohedral twin (orthorhombic lattice which emulate tetragonal, i.e, the *a* crystallographic axis is approximately equal to the *b* one) with two domains. The BASF parameter was convergent to the value 0.297(4). All H atoms were either located by Fourier difference maps and refined isotropically or were introduced at calculated positions as riding on bonded atoms. All non-H atoms were refined anisotropically, except of the water solvate molecules in **4**·4H_2O which were found disordered and refined isotropically with fixed occupation factors.

2.4. Biological assays

2.4.1. Cell culture

LMS (leiomyosarcoma), MCF-7 (human breast cancer) and MRC-5 (normal human fetal lung fibroblast) cell lines were used in this study [28]. Cells were cultured in Dulbecco's modified Eagle's medium (DMEM), supplemented with 10% fetal bovine serum, 1% penicillin/streptomycin and 0.5% L-glutamine (1% L-glutamine for the culture of the MRC-5 cells) at 37 °C in a humidified with 5% CO_2 incubator. The average IC_{50} value (concentration required for 50% inhibition of cell growth) was determined from the curve of inhibiting percentage versus dose.

Table 1
Crystallographic data for complexes **3** and **4**·4H_2O.

Parameter	**3**	**4**·4H_2O
Empirical formula	$C_{18}H_{22}ZnN_8O_{10}$	$C_{14}H_{26}ZnN_{12}O_{14}$
M (g mol^{-1})	575.81	651.84
Crystal dimensions (mm)	0.02 × 0.28 × 0.28	0.26 × 0.26 × 0.24
Crystal system	orthorhombic	orthorhombic
Space group	*P*2(1)2(1)2(1)	*P*2(1)2(1)2(1)
Unit cell dimensions		
α (Å)	7.4582(2)	7.0635(1)
b (Å)	7.4654(2)	7.0866(1)
c (Å)	41.4496(12)	50.747(1)
α (°)	90	90
β (°)	90	90
γ (°)	90	90
V (Å^3)	2307.85(11)	2540.20(8)
Z	4	4
ρ_{calc} (g cm^{-3})	1.657	1.704
Radiation, λ (Å) Cu Kα	1.54178	1.54178
T (K)	293(2)	180(2)
$2\theta_{max}$ (°)	130.00	130.00
μ (mm^{-1})	2.140	2.188
F(000)	1184	1344
Total reflections	8294	17566
Unique reflections (R_{int})	3480 (0.0564)	16957 (0.0482)
Data with $I > 2\sigma(I)$	2971	3995
Parameters refined	335	415
$(\Delta\rho)_{max}/(\Delta\rho)_{min}$ (e Å^{-3})	1.032 and −0.980	0.609 and −0.779
Goodness-of-fit (GOF) on F^2	1.158	1.051
R_1,[a] wR_2[b] ($I > 2\sigma(I)$)	0.0833, 0.2051	0.0475, 0.1108

[a] $R_1 = \Sigma(|F_o|-|F_c|)/\Sigma(|F_o|)$.
[b] $wR_2 = \{\Sigma[w(F_o^2-F_c^2)^2]/\Sigma[w(F_o^2)^2]\}^{1/2}$.

2.4.2. MTT assay

Cell growth inhibition was analyzed using the MTT assay. Briefly, 5×10^3 of LMS or MCF-7 cells and 7×10^3 of MRC-5 cells were cultured overnight on 96-well plates and media containing different concentrations of the complexes **1**–**4**, dissolved in DMSO, were added. After incubation for 48 h, 50 μL of MTT were added in each well from a stock solution (2 mg/mL), and incubated for an additional 3 h. Then, 200 μL of DMSO were added in each well and mixed gently with a multi-channel pipette. Purple formazans were eluted and absorbance was determined at 540 nm (background absorbance measured at 690 nm) using a microplate spectrophotometer (DigiScan Reader 400, ASYS Hitech GmbH, Austria). All experiments were performed in triplicate.

2.4.3. Colony efficiency

LMS cells were seeded into 24-well plates at a density of 2×10^4 cells per well and incubated for 24 h. Media containing different concentrations of the complexes **1**–**4**, dissolved in DMSO, were added. After 48 h of incubation, cells were washed with PBS, detached with trypsin and a standard number of 600 (for LMS) or 1200 (for MCF-7) cells per sample were re-seeded into a well of a six-well plate. All re-cultures were allowed to growth up to 168 h. Then, cells were washed twice with PBS, fixed with a mixture of acetic acid:methanol at a ratio of 3:1, stained with Giemsa solution (diluted in tap water at a ratio 1:10) and let to dry at room temperature. Each sample was performed in triplicate and the total number of stained-formed colonies was recorded.

2.4.4. Flow cytometry

Six-well plates were used for the determination of apoptosis. LMS cells were seeded at a density of 6×10^4 cells per well and incubated for 24 h before the experiment. Cells were washed twice with PBS and treated with media containing various concentrations of the complexes **1**–**4** dissolved in DMSO. Supernatants and cells (detached by trypsinization) were collected, centrifuged and cell pellets were suspended in calcium buffer 1× at a rate 10^5 cells/100 μL. Then, cells from each sample were stained with 5 μL of Annexin V-Fluorescein isothiocynate (FITC) and 4 μL of Propidium Iodide (PI) and incubated for 15 min in the dark at room temperature. DNA content was determined on a fluorescence-activated cell sorting flow cytometer (Partec ML, Partec GmbH, Germany). Percentage of apoptotic (early and late) and necrotic cells was calculated over all viable cells (100%) [29].

2.4.5. Antibacterial activity

The antibacterial activity of complexes **1**–**4** was tested against *Escherichia coli* DH5a, *Zymomonas mobilis* NCIB 11163, *Streptococcus thermophilus* LMG 18311 and *Corynebacterium glutamicum* ATCC 21253 by measuring the minimum inhibitory concentration (MIC) [30]. *E. coli* and *C. glutamicum* were grown in LB (1% tryptone, 1% sodium chloride, 0.5% yeast extract) with agitation at 37 °C and 30 °C, respectively. *Z. mobilis* was grown at 30 °C without agitation in a complete medium consisting of 2% glucose, 0.1% potassium dihydrogen phosphate, 0.1% ammonium sulfate, 0.05% magnesium sulfate and 0.5% yeast extract. *S. thermophilus* was grown in M17 broth (0.25% tryptic digest of casein, 0.25% peptone, 0.5% soy peptone, 0.25% yeast extract, 0.5% beef extract, 1.9% sodium glycerophosphate, 0.025% magnesium sulfate, 0.05% ascorbic acid, 0.5% lactose) at 37 °C with agitation. The complexes were dissolved in DMSO and tested at final concentrations ranging from 3–200 μM.

Control cultures in the absence of the studied compounds, as well as in the presence of DMSO were also carried out. All tests were performed at least in duplicate.

Cultures of each bacterial strain were prepared by using an overnight culture as inoculum at a dilution of 1:20. The complexes were added at final concentrations of 3, 6, 12, 20 (or 25) μM, 50, 100, 150 and 200 μM. The bacterial growth was monitored by measuring the absorbance at 600 nm of the culture after 12 and 24 h. In case a certain concentration of a complex did not allow growth of the bacterial strain, the procedure was repeated by reducing the complex concentration in half, until reaching the one permitting normal cell growth. The concentration in which bacterial cells show no growth represents the MIC value [30].

2.5. Statistical analysis

Data are expressed as mean ± SD. The statistical significance between data means was determined by Student's *t*-test (SPSS version 16.0, Statistical Package for the Social Sciences software, SPSS, Chicago, USA). *p*-Values < 0.05 were considered as significant.

3. Results and discussion

3.1. Synthetic comments

Many synthetic procedures [31] to oligo- and polynuclear 3d-metal complexes rely on the reactions of metal carboxylate or β-diketonate starting materials, such as $M(O_2CR)_2$ or $M(RCOCHCOR)_2$ (R = various), respectively, with a potentially chelating/bridging ligand. This route was also known from our previous work to yield structurally interesting Zn^{II} complexes using several 2-pyridyl oxime ligands [32]. In the present study we have investigated the reactions between the relatively unexplored 2-pyridyl oxime ligand, namely pyridine-2-amidoxime (ampaoH), and two pyridyl-based dioximes, namely 2,6-diacetylpyridine dioxime ($dapdoH_2$) and pyridine-2,6-diamidoxime ($dampdoH_2$), with simple Zn^{II} carboxylate and non-carboxylate sources.

Various reactions have been systematically explored with differing reagent ratios, reaction solvents, and other conditions. As previously reported, the reaction of $Zn(O_2CMe)_2{\cdot}2H_2O$ or $Zn(O_2CPh)_2{\cdot}2H_2O$ with ampaoH in a 1:2 molar ratio in MeOH gave a colorless solution and the subsequent isolation of well-formed colorless crystals of the complexes $[Zn(O_2CMe)_2(ampaoH)_2]$ (**1**) and $[Zn(O_2CPh)_2(ampaoH)_2]$ (**2**), respectively, in fairly good yields (50–80%). In an attempt to investigate the reactions of various Zn(II) non-carboxylate sources with pyridyl dioxime ligands, we performed the 1:2 reaction between $Zn(NO_3)_2{\cdot}4H_2O$ and $dapdoH_2$ in MeOH. The colorless solution obtained led to the subsequent isolation of well-formed colorless crystals of $[Zn(dapdoH_2)_2](NO_3)_2$ (**3**) in excellent yield (~85%) upon layering of the reaction solution with Et_2O. When the same reaction and crystallization process was repeated using $dampdoH_2$ in place of $dapdoH_2$, complex $[Zn(dampdoH_2)_2](NO_3)_2{\cdot}4H_2O$ (**4**·$4H_2O$) was isolated as colorless crystals in good yield (~65%).

Despite our efforts, no zinc(II) complexes containing the mono- and/or dianionic forms of the pyridyl dioxime ligands could be obtained by employing basic conditions. Increase in the $Zn(NO_3)_2$/$dapdoH_2$ (or $dampdoH_2$) ratio to 1:1 still gives complexes **3** and **4**, but in lower yields of 20–25% (depending on the pyridyl dioxime used). Complexes **3** and **4** were also obtained when the corresponding reactions were performed in MeCN, EtOH or $MeNO_2$, but in much lower yields (~30–35%), whereas no significant reactions were observed when the solvent was CH_2Cl_2 or $CHCl_3$. All complexes **1**–**4** are stable solids at room temperature, and non-sensitive toward air and moisture. They are soluble in dimethylformamide, dimethylsulfoxide and H_2O, and insoluble in almost all common organic solvents such as chloroform, benzene, toluene, etc.

3.2. Description of structures

The molecular structures of the cations of complexes **3** and **4** are depicted in Figs. 2 and 3, respectively. Selected interatomic distances and angles are listed in Tables 2 and 3.

Complex **3** crystallizes in the orthorhombic space group $P2_12_12_1$. Its structure consists of $[Zn(dapdoH_2)_2]^{2+}$ cations (Fig. 2) and NO_3^- anions. The Zn^{II} center is coordinated by two *N*,*N*′,*N*″-tridentate chelating (η^3) $dapdoH_2$ ligands. The $dapdoH_2$ donor atoms are the nitrogen atoms of the two neutral oxime and the pyridyl groups. Thus, the Zn^{II} atom is six-coordinate with a distorted octahedral N_6 environment. The main distortion from octahedral geometry is due to the small bite angles of the $dapdoH_2$ chelates (average value 74.9°). The pyridyl nitrogen atoms can be viewed as strongly coordinating to the metal [Zn(1)–N(2) = 2.023(8)/Zn(1)–N(12) = 2.024(8) Å] in the axial direction (N(2)–Zn(1)–N(12) = 176.0(4)°), while the four oximato-type nitrogen atoms of the equatorial plane form weaker bonds to Zn^{II} [Zn(1)–N(1) = 2.240(13)/Zn(1)–N(3) = 2.225(12)/Zn(1)–N(11) = 2.262(9)/Zn(1)–N(13) = 2.211(10) Å].

The pyridyl rings of the two $dapdoH_2$ ligands are planar and almost perfectly perpendicular to each other, forming an angle of 89.4° [N(2)C(3)C(4)C(5)C(6)C(7)/N(12)C(13)C(14)C(15)C(16)C(17)]. The four five-membered chelating rings, Zn(1)–N(1)–C(2)–C(3)–N(2)/Zn(1)–N(2)–C(7)–C(8)–N(3) and Zn(1)–N(11)–C(12)–C(13)–N(12)/Zn(1)–N(12)–C(17)–C(18)–N(13), share the common Zn(1)–N(2) and Zn(1)–N(12) edges. The dihedral angles formed between the mean planes Zn(1)–N(1)–C(2)–C(3)–N(2) and Zn(1)–

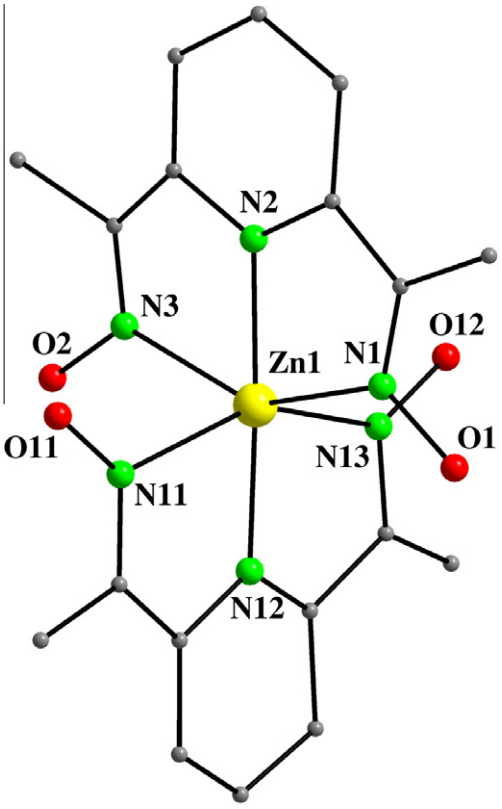

Fig. 2. Partially labeled plot of the cation of **3**, with H atoms omitted for clarity. Color scheme: Zn^{II}, yellow; O, red; N, green; C, gray. (For interpretation of the references to color in this figure legend, the reader is referred to the web version of this article.)

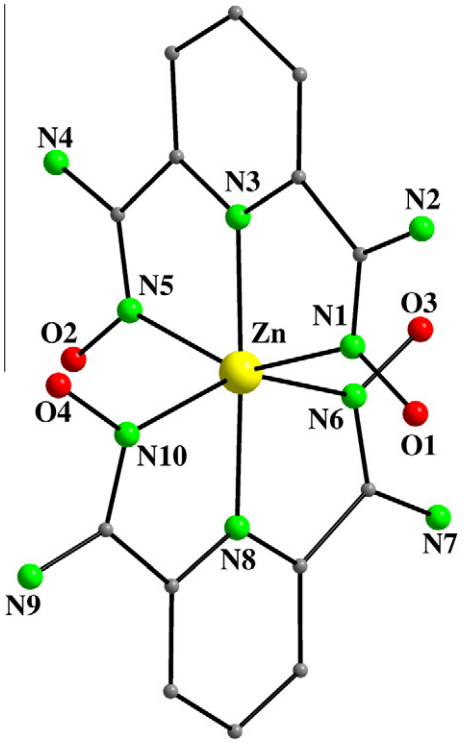

Fig. 3. Partially labeled plot of the cation of **4**, with H atoms omitted for clarity. Color scheme: Zn^{II}, yellow; O, red; N, green; C, gray. (For interpretation of the references to color in this figure legend, the reader is referred to the web version of this article.)

Table 2
Interatomic distances (Å) and angles (°) for complex **3**.

Bond lengths			
Zn(1)-N(1)	2.240(13)	Zn(1)–N(11)	2.262(9)
Zn(1)–N(2)	2.023(8)	Zn(1)–N(12)	2.024(8)
Zn(1)–N(3)	2.225(12)	Zn(1)–N(13)	2.211(10)
Bond angles			
N(1)–Zn(1)–N(2)	74.3(4)	N(2)–Zn(1)–N(13)	107.9(4)
N(1)–Zn(1)–N(3)	149.8(4)	N(3)–Zn(1)–N(11)	94.1(4)
N(1)–Zn(1)–N(11)	92.9(4)	N(3)–Zn(1)–N(12)	105.9(4)
N(1)–Zn(1)–N(12)	104.3(4)	N(3)–Zn(1)–N(13)	94.6(4)
N(1)–Zn(1)–N(13)	93.9(4)	N(11)–Zn(1)–N(12)	73.9(4)
N(2)–Zn(1)–N(3)	75.5(4)	N(11)–Zn(1)–N(13)	149.7(4)
N(2)–Zn(1)–N(11)	102.4(4)	N(12)–Zn(1)-N(13)	75.8(4)
N(2)–Zn(1)–N(12)	176.0(4)		
Intermolecular hydrogen bonds			
Donor···acceptor[a]			D···A
O(11′)···O(22)			2.642
O(12)···O(23)			2.667
O(1″)···O(31)			2.697
O(2)···O(33)			2.647

[a] Symmetry operations to generate equivalent atoms: (′): 1 + *x*, *y*, *z*; (″): *x*, 1 + *y*, *z*.

N(2)–C(7)–C(8)–N(3), and Zn(1)–N(11)–C(12)–C(13)–N(12) and Zn(1)–N(12)–C(17)–C(18)–N(13), are 3.6° and 2.7°, respectively. There are four interionic OH···O hydrogen bonds involving the protonated $dapdoH_2$ O atoms as donors and NO_3^- counterion O atoms as the acceptors. Their dimensions are listed in Table 2. These H bonds serve to bridge neighboring Zn^{II} monomers through NO_3^- counterions, forming in the crystal a 2D H-bonded network extended parallel to the *ab* plane (Fig. 4).

Complex **4**·$4H_2O$ crystallizes in the orthorhombic space group $P2_12_12_1$. The asymmetric unit contains $[Zn(dampdoH_2)_2]^{2+}$ cations, NO_3^- anions and water solvate molecules. The molecular structure of the cation of **4** (Fig. 3) is very similar to that of **3**, with the main

Table 3
Interatomic distances (Å) and angles (°) for complex **4**·$4H_2O$.

Bond lengths			
Zn–N(1)	2.159(5)	Zn–N(6)	2.174(6)
Zn–N(3)	2.080(5)	Zn–N(8)	2.084(5)
Zn–N(5)	2.164(5)	Zn–N(10)	2.168(5)
Bond angles			
N(1)–Zn–N(3)	74.3(2)	N(3)–Zn–N(10)	104.5(2)
N(1)–Zn–N(5)	148.6(2)	N(5)–Zn–N(6)	93.5(2)
N(1)–Zn–N(6)	94.0(2)	N(5)–Zn–N(8)	103.2(2)
N(1)–Zn–N(8)	108.2(2)	N(5)–Zn–N(10)	93.9(2)
N(1)–Zn–N(10)	95.1(2)	N(6)–Zn–N(8)	74.6(2)
N(3)–Zn–N(5)	74.3(2)	N(6)–Zn–N(10)	149.3(2)
N(3)–Zn–N(6)	106.3(2)	N(8)–Zn–N(10)	74.6(2)
N(3)–Zn–N(8)	177.4(2)		
Intermolecular hydrogen bonds			
Donor···acceptor[a]			D···A
O(1)···O(33)			2.674
O(2′)···O(31)			2.824
O(4)···O(22)			2.707
O(3″)···O(23)			2.785
N(2)···O(2w)			3.060
N(2)···O(4)			3.126
N(4)···O(3w)			2.971
N(4)···O(23)			3.038
N(7)···O(33)			3.133
N(9)···O(1w)			3.086
N(9)···O(2)			3.144
O(1w)···O(32)			3.146
O(1w)···O(4w)			2.756
O(2w)···O(22)			2.854
O(2w)···O(3w)			2.746
O(3w)···O(21)			2.835
O(3w)···O(2w)			2.737
O(4w)···O(1w)			2.743

[a] Symmetry operations to generate equivalent atoms: (′): 1 + *x*, *y*, *z*; (″): *x*, 1 + *y*, *z*.

difference located at the type of the neutral pyridyl dioxime ligand ($dampdoH_2$ in **4** versus. $dapdoH_2$ in **3**). Above all, the major difference between the crystal structures of **3** and **4**·$4H_2O$ is the nature of the intermolecular hydrogen bonds which create a 3D framework (Table 3) in the latter. Such 3D framework is built by a 2D layer, which consists of hydrogen bonded neighboring Zn^{II} monomers through NO_3^- counterions and the protonated $dampdoH_2$ O atoms, in a similar way as in complex **3** (four first hydrogen bonds listed in Table 3). With the further involvement of the amino N atoms of each $dampdoH_2$ ligand and the lattice solvate water molecules, neighboring 2D layers are linked through additional hydrogen bonds and thus a complicated 3D framework is formed.

Compounds **1**–**4** join a very small family of mono- and polynuclear complexes with pyridine-2-amidoxime [33], 2,6-diacetylpyridine dioxime [24,34] and pyridine-2,6-diamidoxime [25,35] ligands. According to the Cambridge Crystallographic Data Centre (CCDC), complex **4** is the first structurally characterized Zn(II) complex to contain any form (neutral or anionic) of the pyridine-2,6-diamidoxime ligand. In the case of ligand 2,6-diacetylpyridine dioxime, only a previous Zn(II) compound with formula $[ZnCl_2(dapdoH_2)]$ has been reported to date [36], leaving **3** as the second structurally reported compound bearing the neutral form of $dapdoH_2$.

3.3. Spectroscopic studies

The presence of neutral oxime groups in complexes **3** and **4** is manifested by a broad IR band of medium intensity in the 3450–3440 cm^{-1} region, assigned to $\nu(OH)_{oxime}$ [37]. The broadness and relatively low frequency of these bands are both indicative of strong hydrogen bonding (*vide infra*). Several, medium-intensity bands appear in complex **4** at 3350–2860 cm^{-1}. These are assigned to $\nu_{as}(NH_2)$ and $\nu_s(NH_2)$ stretching vibrations, clearly shifting to

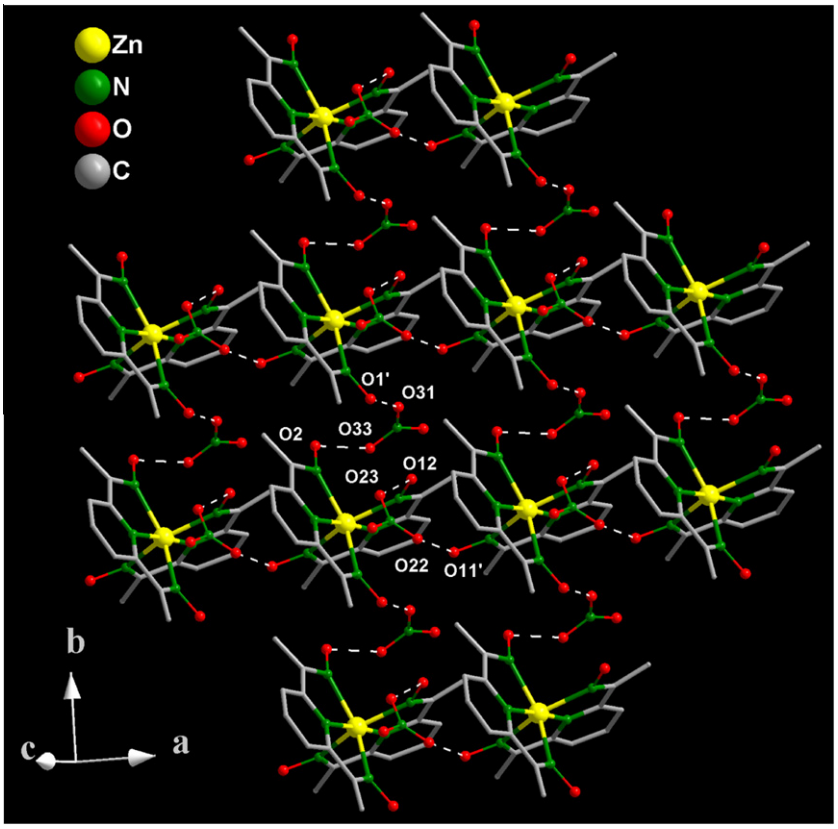

Fig. 4. A section of the 2D hydrogen-bonding network that is present in the crystal structure of complex **3**. Color scheme: Zn^{II}, yellow; O, red; N, green; C, gray. (For interpretation of the references to color in this figure legend, the reader is referred to the web version of this article.)

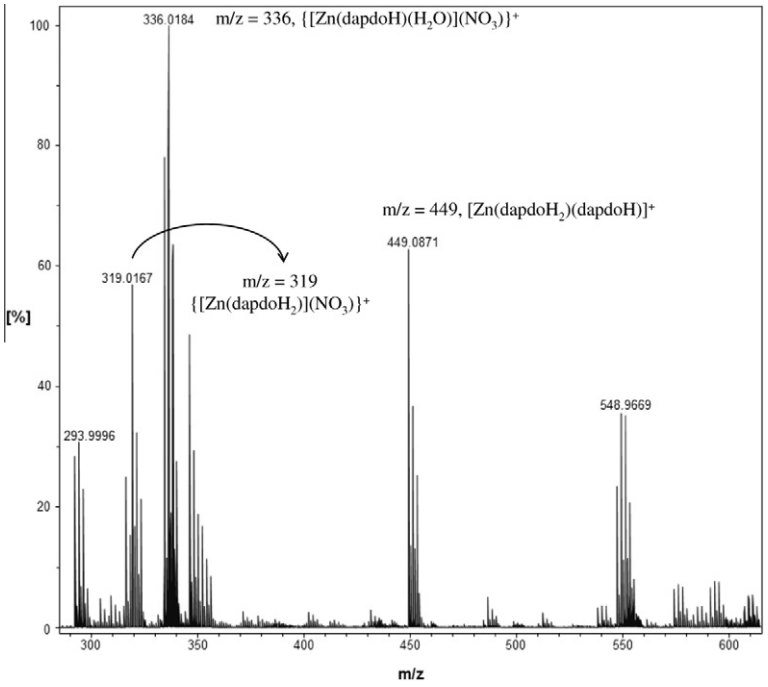

Fig. 5. Positive ESI-MS of complex **3** in DMSO.

lower wavenumbers compared with the corresponding values of the free pyridine-2,6-diamidoxime ligand, due to strong hydrogen-bonding interactions (*vide infra*). Several bands appear in the 1660–1384 cm^{-1} range in the spectra of both **3** and **4**. These are assigned to contributions from the stretching vibrations of the aromatic ring and oxime groups, which overlap with stretches of the nitrate bands; they, thus, do not represent pure vibrations and render exact assignments difficult. The presence of ionic NO_3^- in **3** and

Table 4
IC_{50} values (in μM) of complexes **1**–**4**, and their corresponding metal ion starting materials and free organic ligands against LMS, MCF-7 and MRC-5 cells.

	LMS	MCF-7	MRC-5
Complex **1**	116.6 ± 1.5	137.6 ± 7.1	248.4 ± 6.2
Complex **2**	124.9 ± 1.5	128.5 ± 3.8	245.9 ± 3.6
Complex **3**	5 ± 3.5	7 ± 3.2	31 ± 5.2
Complex **4**	129.1 ± 6.2	105.5 ± 2.7	151.5 ± 4.4
$Zn(O_2CMe)_2$	259.9 ± 5.9	NA	NA
$Zn(O_2CPh)_2$	220.9 ± 5.5	NA	NA
$Zn(NO_3)_2{\cdot}4H_2O$	255.9 ± 8.5	NA	NA
ampaoH	680.3 ± 7.4	NA	NA
$dapdoH_2$	57 ± 11	NA	NA
$dampdoH_2$	742.2 ± 6.9	NA	NA

NA; not available.

4 (established by crystallography) follows from the spectra of these compounds through the appearance of the $\nu_3(E')[\nu_d(NO)]$ mode of the D_{3h} ionic nitrate at ~1384 cm^{-1} [38].

The ^1H and ^{13}C NMR chemical shifts of the free ligands $dapdoH_2$ and $dampdoH_2$ in DMSO-d_6 have been previously reported and discussed in detail [24,39]. The solubilities of the structurally new complexes **3** and **4** in common organic solvents were too low to allow other than DMSO-d_6 solutions to be prepared and studied. In general, the chemical shifts of ligand protons bound to diamagnetic metal ions are influenced by three factors [40]: (i) the electron density on the ligand diminishes upon coordination, inducing a downfield shift; (ii) steric effects lead to a downfield shift; (iii) alignment of a proton above an adjacent aromatic ring leads to a dramatic upfield shift. The ^1H NMR spectra of **3** and **4** were assigned with the aid of recent studies of coordinated $dapdoH_2$ and a number of diamagnetic metal complexes with related ligands [24,39]. As expected, the electron density on the pyridine ring of $dapdoH_2$ and $dampdoH_2$ diminishes upon coordination to the metal centers. Thus, a downfield shift of the pyridine proton resonances is observed for both complexes compared to the free ligands. The effect is greater for the proton in 4-position than for the protons in 3(5)-positions, resulting in a reversal of their relative positions compared to the free ligand [24,39,41]. A relatively large downfield shift is also observed for the oxime proton upon coordination of the metal ion, in agreement with the greater acidity observed for the oxime protons for the metal compounds of $dapdoH_2$ and $dampdoH_2$. Undoubtedly, the ^1H and ^{13}CNMR data for both **3** and **4** confirm their integrity in DMSO solutions.

Positive ion (+) electrospray (ES) mass spectrometry (MS) was used to analyze the new complexes **3** and **4**, dissolved in an aprotic solvent, dimethylsulfoxide, in order to preserve complex integrity while allowing electrospraying. In positive ESI-MS, analyte molecular ions are observed as a result of the addition of a H^+ to the analyte molecule. It is thus common to provide excess of protons by adding small amounts of volatile acids to the sample solution [42]. In the present study, the instability of the compounds under these conditions precluded the use of such an approach. However, even in the absence of charge carriers intense pseudomolecular ions, corresponding to $[Zn(L)_n]^+$ (L is the pyridyl dioxime ligand used each time; n = 1 or 2), were observed for both analyzed complexes **3** and **4** (Fig. 5 shows the representative positive ESI-MS for complex **3**). In support of the assignments shown in Fig. 5 is the

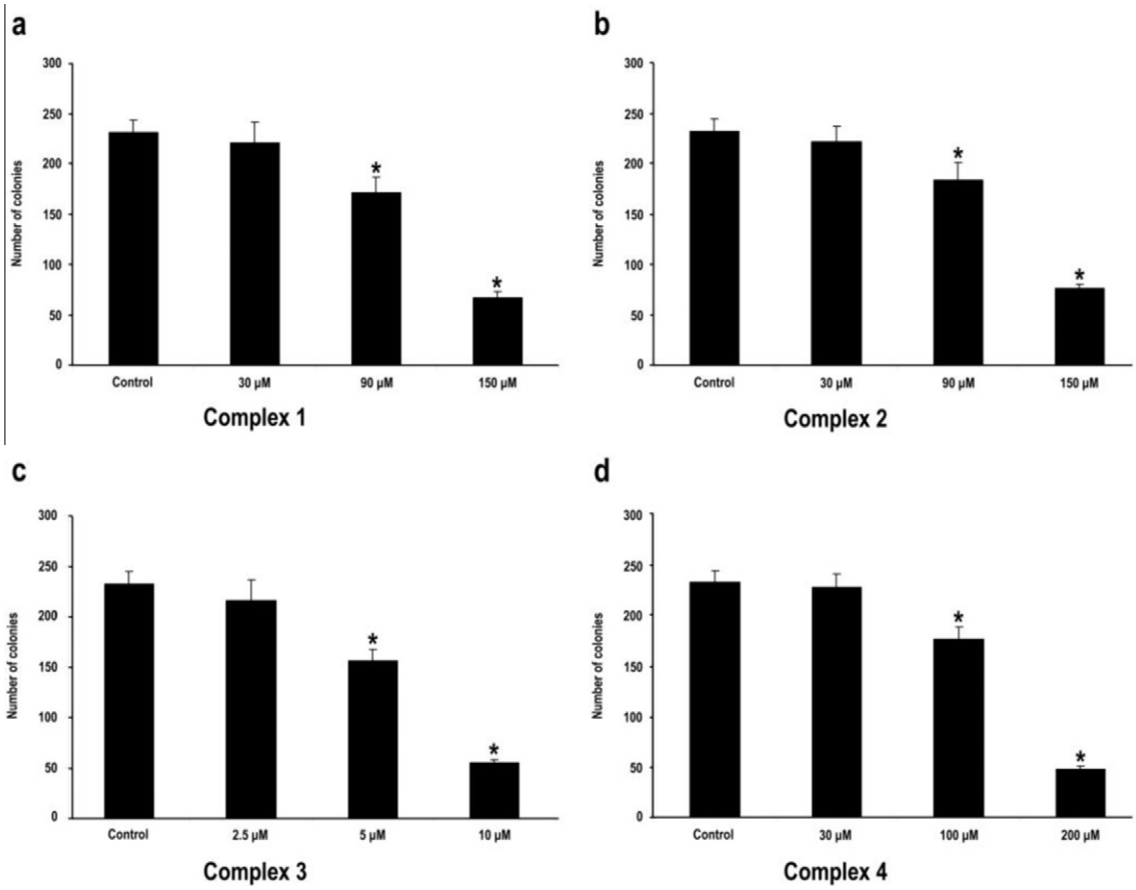

Fig. 6. Colony efficiency of LMS cells treated with IC_{50} or higher concentrations of complexes **1**–**4**.

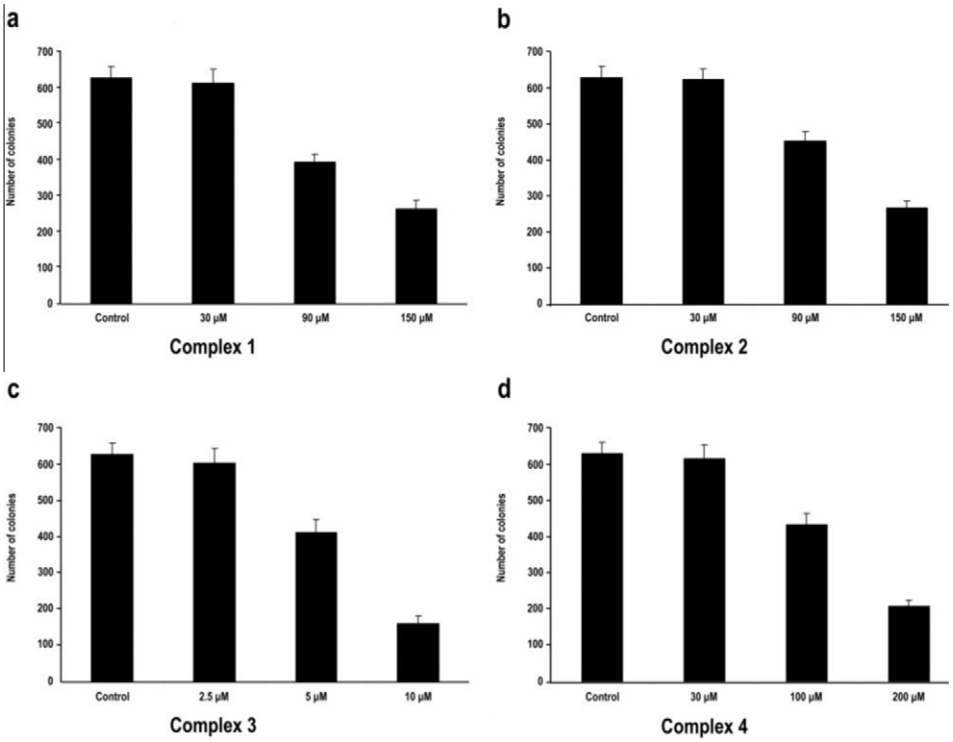

Fig. 7. Colony efficiency of MCF-7 cells treated with IC_{50} or higher concentrations of complexes **1**–**4**.

excellent match observed between the acquired distinct isotopic distributions for the $[Zn(L)_n]^+$ ions and the theoretically calculated distributions. It was also observed for both **3** and **4**, low intensity ion signals attributed (i.e. for the representative compound **3**) to $\{[Zn(dapdo)]\text{-}K\}^+$ ($m/z = 294$) and $\{[Zn(dapdoH_2)(dapdoH)](NO_3)\text{-}K\}^+$ ($m/z = 549$) adduct ions. The presence of the potassium ions is likely due to the solvent and reagent impurities [42].

3.4. Biological studies

3.4.1. Cytotoxic activity

The IC_{50} values for cell growth proliferation for complex **1** against LMS, MCF-7 and MRC-5 cells were 116.6 ± 1.5, 137.6 ± 7.1 and 248.4 ± 6.2 μM, respectively. For complex **2**, the IC_{50} values were 124.9 ± 1.5, 128.5 ± 3.8 μM and 245.9 ± 3.6 μM, while for compound **3** the values were 5 ± 3.5, 7 ± 3.2, 31 ± 5.2 μM against LMS, MCF-7 and MRC-5 cells, respectively. Finally, complex **4** presented cytotoxicity against LMS, MCF-7 and MRC-5 cells with the IC_{50} values being 129.1 ± 6.2, 105.5 ± 2.7 and 151.5 ± 4.4 μM, respectively. Furthermore, cell growth proliferation for the metal ion starting materials and the free organic ligands, was also tested. The IC_{50} values for the starting reagents $Zn(O_2CMe)_2$ (for **1**), $Zn(O_2CPh)_2$ (for **2**) and $Zn(NO_3)_2{\cdot}4H_2O$ (for the structurally new **3** and **4**) against LMS cells were 259.9 ± 5.9, 220.9 ± 5.5 and 255.9 ± 8.5 μM, respectively, whereas for the free organic ligands ampaoH (for complexes **1** and **2**), $dapdoH_2$ (for **3**) and $dampdoH_2$ (for **4**) were 680.3 ± 7.4, 57 ± 11, and 742.2 ± 6.9 μM, respectively. Thus, the observed cytotoxicity of complexes **1**–**4** is not due to their corresponding metal starting materials and free organic ligands. According to the IC_{50} values, complex **3** presents the strongest cytotoxic activity among all complexes, against these two cancer cell lines. It is important to mention that none of the reported complexes presented cytotoxicity on MRC-5 cells, at the corresponding IC_{50} values of the two cancer cell lines (Table 4).

3.4.2. Colony efficiency

The experiments for cell recovery (the ability of treated cells to grow after drug withdrawal-colony efficiency) showed that LMS (Fig. 6) and MCF-7 (Fig. 7) cells, when treated with increasing concentrations of the complexes **1**–**4**, lose their ability to proliferate and growth arrest was irreversible ($p < 0.05$).

3.4.3. Flow cytometry analysis

Untreated cells (control) showed a total background cell death at a percentage of 13.72% (both apoptotic and necrotic cells). The percentage of apoptotic cells (early apoptotic cells Ann+/PI- and late apoptotic cells Ann+/PI+), after 48 h of incubation with complex **1,** was 37.66% and 94.97% at concentrations of 100 and 200 μM, respectively. In comparison, the percentage of necrotic cells, at the same concentrations as previously reported for complex **1**, was 1.6% and 0.38%, respectively. Complex **2** caused apoptosis at a percentage of 25.77% and 44.24% and necrosis at a percentage of 6.57% and 16.33%, at concentrations of 100 and 150 μM, respectively. Complex **3** presented apoptosis at a percentage of 30.56% and 36% when cells treated with 5 and 10 μM, respectively. Additionally, when LMS cells were treated with 150 and 200 μM of complex **4** showed 52.84% and 91.79% of apoptosis, respectively, while the percentages of necrotic cells were negligible. Thus, all complexes **1**–**4** caused a dose-dependent apoptotic cell death against LMS cells (Fig. 8).

3.4.4. Antibacterial activity

The antibacterial activity of the complexes and related substitutes against *E. coli*, *Z. mobilis* and *C. glutamicum* is presented in Table 5. According to the MIC values it is shown that the free ligands $ampaoH_2$ and $dampdoH_2$, and their corresponding compounds **1**/**2** and **4**, do not inhibit growth of the bacteria tested. *C. glutamicum* showed a slightly reduced growth in presence of **1** and **2** at the concentration of 200 μM.

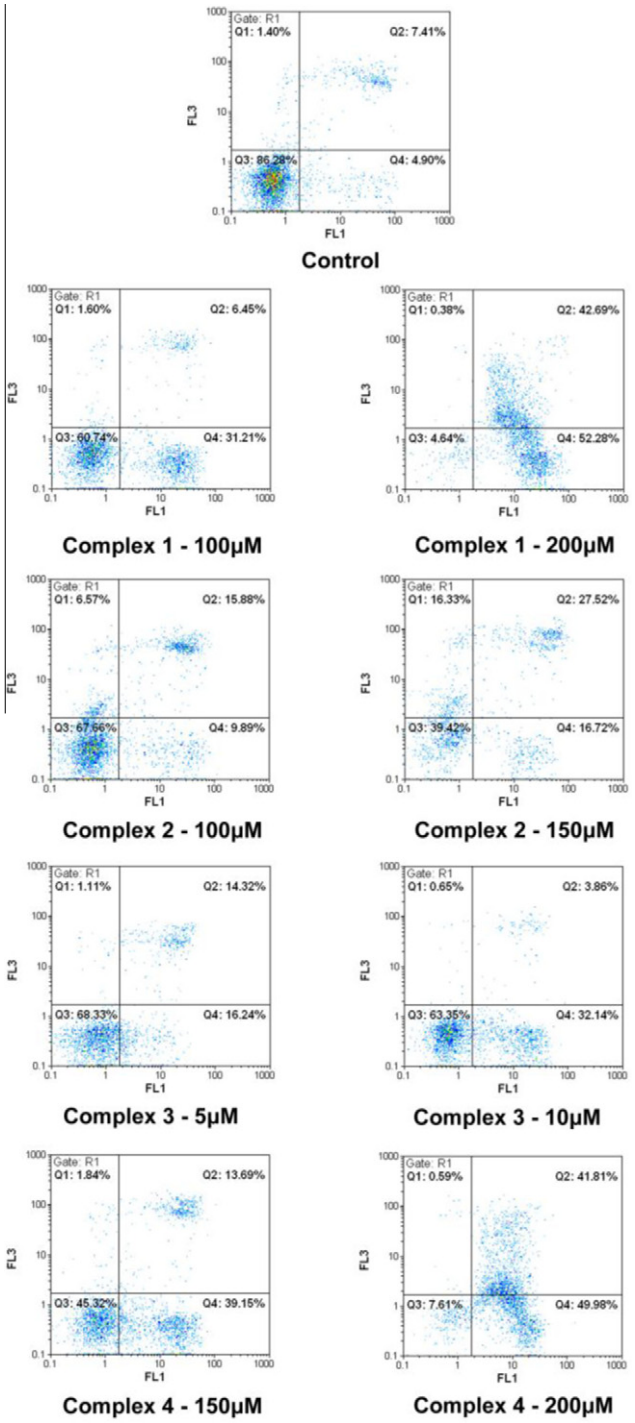

Fig. 8. LMS cells were treated with increasing concentrations of the reported compounds **1**–**4**. Cells were stained with Annexin V-FITC and PI for detection of apoptosis by FACS analysis.

The presence of the free ligand dapdoH_2 and its complex **3** in the growth medium caused a strong inhibition in *Z. mobilis* growth (MIC 25 μM for both compounds), while only a slight growth delay in the cases of *E. coli* and *C. glutamicum*.

The growth of *S. thermophilus* was reduced in the presence of DMSO and therefore is not included in Table 5. However, it is worth mentioning that growth was completely inhibited in the presence of dapdoH_2 at a MIC of 200 μM, and **1** and **3** at a MIC of 200 and 100 μM, respectively.

Table 5
Antibacterial activity of the tested compounds in MIC (μM).

	Gram-		Gram+
	E. coli	*Z. mobilis*	*C. glutamicum*
ampaoH_2	>200	>200	>200
dapdoH_2	>200*	25	>200*
dampdoH_2	>200	>200	>200
Complex **1**	>200	>200	>200*
Complex **2**	>200	>200	>200*
Complex **3**	>200*	25	>200*
Complex **4**	>200	>200	>200

* Slightly reduced growth at 200 μM.

4. Conclusions and perspectives

The present work extends the body of results that emphasize the ability of pyridyl monoximes and pyridyl dioximes to form interesting 3d-metal complexes, not only ones possessing high-nuclearities and impressive magnetic and optical properties, but also compounds with unexplored biological perspectives. The biological studies of the structurally known compounds [Zn(O_2CMe)$_2$(ampaoH)$_2$] (**1**) and [Zn(O_2CPh)$_2$(ampaoH)$_2$] (**2**), where ampaoH is pyridine-2-amidoxime, have been adequately performed. Further, the reactions between Zn(NO_3)$_2$·4H_2O and 2,6-diacetylpyridine dioxime (dapdoH_2) or pyridine-2,6-diamidoxime (dampdoH_2) have provided access to the mononuclear, cationic complexes [Zn(dapdoH_2)$_2$](NO_3)$_2$ (**3**) and [Zn(dampdoH_2)$_2$](NO_3)$_2$ (**4**), both including two *N*,*N*′,*N*″-tridentate chelating (η^3) pyridyl dioxime ligands. From a structural viewpoint, complex **4** is the first structurally characterized Zn(II) compound to contain any form (neutral or anionic) of the dampdoH_2 ligand, whereas **3** is only the second structurally reported Zn(II) complex bearing the neutral form of dapdoH_2, albeit the first biologically studied. The detailed spectroscopic and physicochemical characterization of all four compounds with a variety of techniques revealed their integrity in DMSO solutions.

The *in vitro* experiments revealed that the Zn(II) starting materials present similar cytotoxic activity against LMS cells. Complex **3** presents the highest cytotoxic activity against LMS and MCF-7 cells, among the other three complexes. It is believed that the potent cytotoxicity of complex **3** is due to the presence of the coordinated dapdoH_2 ligand, the latter presenting the strongest cytotoxicity compared to those of the other two organic ligands, namely the ampaoH and dampdoH_2. Additionally, all complexes showed mild toxicity against MRC-5 cells. The LMS and MCF-7 cells lost their ability to proliferate and growth arrest was irreversible, when treated with increasing concentrations of the complexes **1**–**4**. Flow cytometry analysis showed that all complexes cause apoptosis to LMS cells, at a dose-dependent manner. Note that metal complexes, including Zn(II) ones, can inhibit topoisomerase I, which is over-expressed in MCF-7 cells [43,44]. It is possible that the reported compounds **1**–**4** lead the cancer cells to apoptoptic death via the same pathway. Moreover, Zn(II) complexes, as described preciously, have antidiabetic and insulin-mimetic properties. Preliminary studies on the metabolism of the cancer cells, used in our experiments, indicate that such complexes play a key role in the inhibition of glycolysis, the major metabolic pathway, wherein cancer cells use to produce ATP [45,46]. Further studies are needed to completely understand the mechanism of action and the structure-related activity of the reported metal complexes. Finally, complexes **1**, **2** and **4** do not present antibacterial activity against *E. coli*, *Z. mobilis* and *C. glutamicum*, while complex **3** presents inhibition in *Z. mobilis* and slight growth delay to *E. coli* and *C. glutamicum*, but this inhibition is close to that presented by its coordinated ligand.

We have no reason to believe that this research area is exhausted of new results. Indeed, ongoing studies are producing additional and interesting products, and our belief is that we have scratched only the surface of the coordination chemistry of zinc(II) based on pyridyl mono- and dioxime ligands. As far as future perspectives are concerned, analogues of **1**–**4** with other pyridyl mono- and dioximes are not known to date, and it is currently not evident whether the preparation and stability of Zn(II) complexes are dependent on the particular nature of the R substituent on the oxime carbon.

Acknowledgments

Th.C.S. thanks the Royal Society of Chemistry Research Fund for chemical supply. K.F.K. and E.M.-Z. thank the Research Committee of the University of Patras for funding this work (C. Karatheodori Grant 2008, No. C584). The authors wish to thank Prof. G. Stephanopoulos (MIT) for providing *C. glutamicum* ATCC 21253.

Appendix A. Supplementary material

CCDC 816765 (**1**·2MeOH), 816766 (**2**·0.5H_2O), 881212 (**3**), and 881213 (**4**·4H_2O) contain the supplementary crystallographic data for this paper. These data can be obtained free of charge from The Cambridge Crystallographic Data Centre via www.ccdc.cam.ac.uk/data_request/cif.

Supplementary data associated with this article can be found, in the online version, at http://dx.doi.org/10.1016/j.ica.2012.09.039.

References

[1] A.J.L. Pombeiro, V.Yu. Kukushkin, in: J.A. McCleverty, T.J. Meyer (Eds.), Comprehensive Coordination Chemistry II, vol. 1, Elsevier, Amsterdam, 2004, p. 631.
[2] P. Eyer, Toxicol. Rev. 22 (2003) 165–190.
[3] R.M. Black, J.M. Harrison, The chemistry of organophosphorus chemical warfare Agents, in: F.R. Hartley (Ed.), The Chemistry of Organophosphorus Compounds, vol. 4, John Wiley & Sons, Chichester, 1996, pp. 781–840.
[4] J. Bajgar, Adv. Clin. Chem. 38 (2004) 151–216.
[5] (a) K. Kuca, D. Jun, K. Musilek, Mini-Rev. Med. Chem. 6 (2006) 269;
(b) K. Musilek, M. Dolezal, F. Gunn-Moore, K. Kuca, Med. Res. Rev. 31 (2011) 548.
[6] E. Abele, R. Abele, E. Lukecics, Chem. Heterocycl. Compd. 39 (2003) 825.
[7] For an excellent review, see: (a) P. Chaudhuri, Coord. Chem. Rev. 243 (2003) 143;;
. For a comprehensive review, see:(b) C.J. Milios, Th.C. Stamatatos, S.P. Perlepes, Polyhedron 25 (2006) 134 (Polyhedron Report);
For an excellent review, see: (c) C.J. Milios, S. Piligkos, E.K. Brechin, Dalton Trans. (2008) 1809 (Dalton Perspective).
[8] M. Prinz, K. Kuepper, C. Taubitz, M. Raekers, S. Khanra, B. Biswas, T. Weyhermüller, M. Uhlarz, J. Wosnitza, J. Schnack, A.V. Postnikov, C. Schröder, S.J. George, M. Neumann, P. Chaudhuri, Inorg. Chem. 49 (2010) 2093;;
(b) B. Biswas, S. Salunke-Gawali, T. Weyhermüller, V. Bachler, E. Bill, P. Chaudhuri, Inorg. Chem. 49 (2010) 626;
(c) B. Biswas, U. Pieper, T. Weyhermuller, P. Chaudhuri, Inorg. Chem. 48 (2009) 6781;
(d) P. Chaudhuri, T. Weyhermüller, R. Wagner, S. Khanra, B. Biswas, E. Bothe, E. Bill, Inorg. Chem. 46 (2007) 9003;
(e) S. Khanra, T. Weyhermüller, E. Bill, P. Chaudhuri, Inorg. Chem. 45 (2006) 5911;
(f) S. Khanra, T. Weyhermüller, E. Rentschler, P. Chaudhuri, Inorg. Chem. 44 (2005) 8176;
(g) S. Ross, T. Weyhermüller, E. Bill, K. Wieghardt, P. Chaudhuri, Inorg. Chem. 40 (2001) 6656;
(h) Th.C. Stamatatos, D. Foguet-Albiol, S.-C. Lee, C.C. Stoumpos, C.P. Raptopoulou, A. Terzis, W. Wernsdorfer, S.O. Hill, S.P. Perlepes, G. Christou, J. Am. Chem. Soc. 129 (2007) 9484;
(i) C.C. Stoumpos, Th.C. Stamatatos, H. Sartzi, O. Roubeau, A.J. Tasiopoulos, V. Nastopoulos, S.J. Teat, G. Christou, S.P. Perlepes, Dalton Trans. (2009) 1004;
(j) Th.C. Stamatatos, A.K. Boudalis, Y. Sanakis, C.P. Raptopoulou, Inorg. Chem. 45 (2006) 7372;
(k) Th.C. Stamatatos, S. Dionyssopoulou, G. Efthymiou, P. Kyritsis, C.P. Raptopoulou, A. Terzis, R. Vicente, A. Escuer, S.P. Perlepes, Inorg. Chem. 44 (2005) 3374;
(l) Th.C. Stamatatos, A. Bell, P. Cooper, A. Terzis, C.P. Raptopoulou, S.L. Heath, R.E.P. Winpenny, S.P. Perlepes, Inorg. Chem. Commun. 8 (2005) 533;
(m) Th.C. Stamatatos, K.A. Abboud, S.P. Perlepes, G. Christou, Dalton Trans. (2007) 3861;
(n) T. Weyhermüller, R. Wagner, S. Khanra, P. Chaudhuri, Dalton Trans. (2005) 2539;
(o) Th.C. Stamatatos, A. Escuer, K.A. Abboud, C.P. Raptopoulou, S.P. Perlepes, G. Christou, Inorg. Chem. 47 (2008) 11825;
(p) Th.C. Stamatatos, E. Diamantopoulou, C.P. Raptopoulou, V. Psycharis, A. Escuer, S.P. Perlepes, Inorg. Chem. 46 (2007) 2350.
[9] R. Breslow, D. Chipman, J. Am. Chem. Soc. 87 (1965) 4195.
[10] R. Breslow, L.E. Overman, J. Am. Chem. Soc. 92 (1970) 1075.
[11] J. Suh, M. Cheong, H. Han, Bioorg. Chem. 12 (1984) 188.
[12] A.K. Yatsimirsky, P. Gómez-Tagle, S. Escalante-Tovar, L. Ruiz-Ramirez, Inorg. Chim. Acta 273 (1998) 167.
[13] N.P. Farell, Uses of Inorganic Chemistry in Medicine, The Royal Society of Chemistry, London, UK, 1999.
[14] (a) A. Misra, S. Ganesh, A. Shahiwala, S.P. Shah, Pharm. Pharm. Sci. 6 (2003) 252;
(b) W.H. de Jong, P.J.A. Borm, Int. J. Nanomed. 3 (2008) 133.
[15] (a) E. Weder, T.W. Hambley, B.J. Kennedy, P.A. Lay, G.J. Foran, A.M. Rich, Inorg. Chem. 40 (2001) 1295;
(b) Q. Zhou, T.W. Hambley, B.J. Kennedy, P.A. Lay, P. Turner, B. Warwick, J.R. Biffin, H.L. Regtop, Inorg. Chem. 39 (2000) 3742.
[16] H.L. Hellmich, C.J. Frederickson, D.S. DeWitt, R. Saban, M.O. Parsley, R. Stephenson, M. Velasco, T. Uchida, M. Shimamura, D.S. Prough, Neurosci. Lett. 355 (2004) 221.
[17] (a) O. Sánchez-Guadarrama, H. López-Sandoval, F. Sánchez-Bartéz, I. Gracia-Mora, H. Höpfl, N. Barba-Behrens, J. Inorg. Biochem. 103 (2009) 1204;
(b) P.F. Liguori, A. Valentini, M. Palma, A. Bellusci, S. Bernardini, M. Ghedini, M.L. Panno, C. Pettinari, F. Marchetti, A. Crispini, D. Pucci, Dalton Trans. 39 (2010) 4205.
[18] K. Singh, Y. Kumar, P. Puri, C. Sharma, K.R. Aneja, Bioinorg. Chem. Appl. (2011) 901716.
[19] K. Vijayaraghavan, S. Iyyam Pillai, S.P. Subramanian, Eur. J. Pharmacol. 680 (2012) 122.
[20] K.F. Konidaris, R. Papi, E. Katsoulakou, C.P. Raptopoulou, D. Kyriakidis, E. Manessi-Zoupa, Bioinorg. Chem. Appl. (2010) 803424.
[21] M. Alexiou, E. Katsoulakou, C. Dendrinou-Samara, C.P. Raptopoulou, V. Psycharis, E. Manessi-Zoupa, S.P. Perlepes, D.P. Kessissoglou, Eur. J. Inorg. Chem. (2005) 1964.
[22] E. Katsoulakou, N. Lalioti, C.P. Raptopoulou, A. Terzis, E. Manessi-Zoupa, S.P. Perlepes, Inorg. Chem. Commun. 5 (2002) 719.
[23] E. Bernasek, J. Org. Chem. 22 (1957) 1263.
[24] C.W. Glynn, M.M. Turnbull, Transition Met. Chem. 27 (2002) 822.
[25] B.A. Bovenzi, G.A. Pearse, Jr., J. Chem. Soc., Dalton Trans. (1997) 2793.
[26] K.F. Konidaris, V. Bekiari, E. Katsoulakou, C.P. Raptopoulou, V. Psycharis, S.P. Perlepes, Th.C. Stamatatos, E. Manessi-Zoupa, Inorg. Chim. Acta 376 (2011) 470.
[27] (a) Crystal Clear, Rigaku/MSC Inc., The Woodlands, Texas, USA 2005; (b) G.M. Sheldrick, SHELXS-97, Structure Solving Program, University of Göttingen, Germany, 1997; (c) G.M. Sheldrick, SHELXL-97, Program for the Refinement of Crystal Structures from Diffraction Data, University of Göttingen, Germany, 1997.
[28] A. Evangelou, S. Karkabounas, G. Kalpouzos, M. Malamas, R. Liasko, D. Stefanou, A.T. Vlahos, T.A. Kabanos, Cancer Lett. 119 (1997) 221.
[29] Verginadis II, S. Karkabounas, Y. Simos, E. Kontargiris, S.K. Hadjikakou, A. Batistatou, A. Evangelou, K. Charalabopoulos, Eur. J. Pharm. Sci. 42 (2011) 253.
[30] E. Katsoulakou, M. Tiliakos, G. Papaefstathiou, A. Terzis, C. Raptopoulou, G. Geromichalos, K. Papazisis, R. Papi, A. Pantazaki, D. Kyriakidis, P. Cordopatis, E. Manessi-Zoupa, J. Inorg. Biochem. 102 (2008) 1397.
[31] (a) A.J. Tasiopoulos, A. Vinslava, W. Wernsdorfer, K.A. Abboud, G. Christou, Angew. Chem., Int. Ed. 43 (2004) 2117;
(b) T. Liu, Y.-J. Zhang, Z.-M. Wang, S. Gao, J. Am. Chem. Soc. 130 (2008) 130;
(c) C.-F. Lee, D.A. Leigh, R.G. Pritchard, D. Schultz, S.J. Teat, G.A. Timco, R.E.P. Winpenny, Nature 458 (2009) 314;
(d) A. Ferguson, A. Parkin, J. Sanchez-Benitez, K. Kamenev, W. Wernsdorfer, M. Murrie, Chem. Commun. 3473 (2007);
(e) G. Christou, Polyhedron 24 (2005) 2065;
(f) R.E.P. Winpenny, J. Chem. Soc., Dalton Trans. (2002) 1;
(g) Th.C. Stamatatos, G. Christou, Inorg. Chem. 48 (2008) 3308;
(h) G.S. Papaefstathiou, S.P. Perlepes, Comments Inorg. Chem. 23 (2002) 249.
[32] K.F. Konidaris, M. Kaplanis, C.P. Raptopoulou, S.P. Perlepes, E. Manessi-Zoupa, E. Katsoulakou, Polyhedron 28 (2009) 3242.
[33] (a) G.A. Pearse, P.R. Raithby, C.M. Hay, J. Lewis, Polyhedron 8 (1989) 305;
(b) M. Werner, J. Berner, P.G. Jones, Acta Crystallogr., C 52 (1996) 72;
(c) H.-Z. Kou, G.-Y. An, C.-M. Ji, B.-W. Wang, A.-L. Cui, Dalton Trans. 39 (2010) 9604;
(d) C.-M. Ji, H.-M. Yang, C.-C. Zhao, V. Tangoulis, A.-L. Cui, H.-Z. Kou, Cryst. Growth Des. 9 (2009) 4607;
(e) C. Papatriantafyllopoulou, L.F. Jones, T.D. Nguyen, N. Matamoros-Salvador, L. Cunha-Silva, F.A. Almeida Paz, J. Rocha, M. Evangelisti, E.K. Brechin, S.P. Perlepes, Dalton Trans. (2008) 3153;
(f) A.-L. Cui, P. Han, H.-J. Yang, R.-J. Wang, H.-Z. Kou, Acta Crystallogr., C 63 (2007) m560;
(g) G.A. Pearse, P.R. Raithby, J. Lewis, Polyhedron 8 (1989) 301;
(h) M. Näsäkkälä, H. Saarinen, J. Korvenranta, M. Orama, Acta Crystallogr., C 45 (1989) 1514;

(i) R. Costa, N. Barone, C. Gorczycka, E.F. Powers, W. Cupelo, J. Lopez, R.S. Herrick, C.J. Ziegler, J. Organ. Chem. 694 (2009) 2163.
[34] (a) G. Sproul, G.D. Stucky, Inorg. Chem. 12 (1973) 2898;
(b) S. Khanra, T. Weyhermuller, P. Chaudhuri, Dalton Trans. (2008) 4885;
(c) N. Ozdemir, M. Dincer, O. Dayan, B. Cetinkaya, Acta Crystallogr., C 62 (2006) m315;
(d) H. Namli, A.D. Azaz, S. Karabulut, S. Celen, R. Kurtaran, C. Kazak, Transition Met. Chem. 32 (2007) 266;
(e) I.V. Vasilevsky, R.E. Stenkamp, E.C. Lingafelter, V. Schomaker, R.D. Willett, N.J. Rose, Inorg. Chem. 28 (1989) 2619;
(f) K.A. Abboud, R.C. Palenik, G.J. Palenik, Acta Crystallogr., C 50 (1994) 525;
(g) S.K. Singh, S. Sharma, S.D. Dwivedi, R.-Q. Zou, Q. Xu, D.S. Pandey, Inorg. Chem. 47 (2008) 11942;
(h) S. Khanra, T. Weyhermuller, P. Chaudhuri, Dalton Trans. (2007) 4675;
(i) S. Abram, C. Maichle-Mossmer, U. Abram, Polyhedron 16 (1997) 2183;
(j) Th.C. Stamatatos, B.S. Luisi, B. Moulton, G. Christou, Inorg. Chem. 47 (2008) 1134;
(k) S. Abram, C. Maichle-Mossmer, U. Abram, Polyhedron 16 (1997) 2291;
(l) C. Lampropoulos, Th.C. Stamatatos, K.A. Abboud, G. Christou, Inorg. Chem. 48 (2009) 429;
(m) I.V. Vasilevsky, R.E. Stenkamp, E.C. Lingafelter, N.J. Rose, J. Coord. Chem. 19 (1988) 171;
(n) A. Escuer, B. Cordero, X. Solans, M. Font-Bardia, T. Calvet, Eur. J. Inorg. Chem. (2008) 5082;
(o) B.C. Unni Nair, J.E. Sheats, P. Ponteciello, D. Van Engen, V. Petrouleas, G.C. Dismukes, Inorg. Chem. 28 (1989) 1582;
(b) R.E. Marsh, Inorg. Chem. 29 (1990) 572;
(q) A. Escuer, J. Esteban, O. Roubeau, Inorg. Chem. 50 (2011) 8893;
(r) A. Escuer, J. Esteban, N. Aliaga-Alcalde, M. Font-Bardia, T. Calvet, O. Roubeau, S.J. Teat, Inorg. Chem. 49 (2010) 2259.
[35] (a) A. Escuer, G. Vlahopoulou, S.P. Perlepes, M. Font-Bardia, T. Calvet, Dalton Trans. 40 (2011) 225;
(b) M. Salonen, H. Saarinen, I. Mutikainen, J. Coord. Chem. 61 (2008) 1462.
[36] G.A. Nicholson, J.L. Petersen, B.J. McCormick, Inorg. Chem. 21 (1982) 3274.
[37] (a) C.J. Milios, E. Keffalloniti, C.P. Raptopoulou, A. Terzis, A. Escuer, R. Vicente, S.P. Perlepes, Polyhedron 23 (2004) 83;
(b) K.W. Nordquest, D.W. Phelps, W.F. Little, D.J. Hodgson, J. Am. Chem. Soc. 98 (1976) 1104;
(c) C.C. Stoumpos, Th.C. Stamatatos, V. Psycharis, C.P. Raptopoulou, G. Christou, S.P. Perlepes, Polyhedron 27 (2008) 3703.
[38] (a) K. Nakamoto, Infrared and Raman Spectra of Inorganic and Coordination Compounds, fourth ed., Wiley, New York, 1986;
(b) E. Katsoulakou, V. Bekiari, C.P. Raptopoulou, A. Terzis, P. Lianos, E. Manessi-Zoupa, S.P. Perlepes, Spectrochim. Acta, A 61 (2005) 1627.
[39] R. Banks, R.F. Brookes, Chem. Ind. (1974) 617.
[40] H.A. Nieuwenhuis, J.G. Haasnoot, R. Hage, J. Reedijk, T.L. Snoeck, D.J. Stufkens, J.G. Vos, Inorg. Chem. 30 (1991) 48 (and references cited therein).
[41] G.I.H. Hanania, D.H. Irvine, F. Schurauh, J. Chem. Soc. (1965) 1149.
[42] (a) G.J. Sopasis, A.B. Canaj, A. Philippidis, M. Siczek, T. Lis, J.R. O'Brien, M.M. Antonakis, S.A. Pergantis, C.J. Milios, Inorg. Chem. 51 (2012) 5911;
(b) S. Anbu, S. Kamalraj, B. Varghese, J. Muthumary, M. Kandaswamy, Inorg. Chem. 51 (2012) 5580.
[43] S.-T. Von, H.-L. Seng, H.-B. Lee, S.-W. Ng, Y. Kitamura, M. Chikira, C.-H. Ng, J. Biol. Inorg. Chem. 17 (2012) 57.
[44] G. Chashoo, S.K. Singh, P.R. Sharma, D.M. Mondhe, A. Hamid, A. Saxena, S.S. Andotra, B.A. Shah, N.A. Qazi, S.C. Taneja, A.K. Saxena, Chem. Biol. Interact. 189 (2011) 60.
[45] R. Moreno-Sanchez, S. Rodrıguez-Enrıquez, A. Marın-Hernandez, E. Saavedra, FEBS J. 274 (2007) 1393.
[46] A. Ramanathan, C. Wang, S.L. Schreiber, Proc. Natl. Acad. Sci. 102 (2005) 5992.